

Refereed Proceedings

Heat Exchanger Fouling and Cleaning:

Fundamentals and Applications

Engineering Conferences International

Year 2003

Development of a Data-Based Method
for Performance Monitoring of Heat
Exchangers

A. Sawyer
University of Tennessee

E. Eryurek
Emerson Process Management

A. E. Ruggles
University of Tennessee

K. Kavaklioglu
Emerson Process Management

B. R. Upadhyaya
University of Tennessee

J. Miller
Emerson Process Management

DEVELOPMENT OF A DATA-BASED METHOD FOR PERFORMANCE MONITORING OF HEAT EXCHANGERS

A. Sawyer¹, A. E. Ruggles¹, B. R. Upadhyaya¹, E. Eryurek², K. Kavaklioglu² and J. Miller²

¹ University of Tennessee, College of Engineering, Pasqua Engineering Building, Knoxville, Tennessee 37996-2300

² Emerson Process Management, Performance Technologies Division, Eden Prairie, Minnesota, 55344-3620

ABSTRACT

A multivariate analysis method is developed for processing measurements, and for detecting and isolating faults and monitoring performance degradation in heat exchanger control loops. A heat exchanger inside a typical temperature to flow cascade loop is considered. This system includes a constant speed pump with flow control valves, pressure and temperature measurement. A proportional-integral-differential (PID) controller is used to maintain a temperature set point for the exit flow on one side of the exchanger. A thermal-fluid model for the components in the system is developed.

A Fault Detection and Isolation (FDI) rule-base is formulated from results of simulations performed using these models. Measurements from an installed laboratory heat exchanger control loop are also used.

Faults simulated and induced on the physical heat exchanger loop include tube fouling, sensor drift, fluid leakage, unresponsive valves, plugged process lines, and controller errors. The rule base allows the identification of faults in a heat exchanger control loop given suitable process measurements.

INTRODUCTION

The Temperature-to-Flow-Cascade (TFC) control loop is common to many industrial processes. The proper function of these systems is often important to product quality or energy efficiency in chemical process plants and refineries. The fault detection and isolation (FDI) rule base developed herein facilitates timely and accurate identification of system faults. Timely and accurate identification of system faults can be very valuable to those who operate and maintain these facilities.

The general temperature to flow cascade (TFC) involves two fluid streams passing through a heat exchanger. A proportional-integral-differential (PID) controller is used to maintain the exit flow temperature on one side of the heat exchanger by modulating the flow on the other side of the exchanger. The specific system considered herein has a hot water stream delivered by a centrifugal pump through a control valve to the tube side of a conventional shell and tube heat exchanger. The PID controller monitors the exit temperature of the cold water flow on the shell side of the exchanger and modifies the

cold side flow through the control valve to maintain the hot side exit flow near to the prescribed set point.

The pump, heater, valves, heat exchanger, plumbing, controllers, and instrumentation, are modeled using MATLAB/Simulink (© Mathworks). The performance of the model is validated using data from the physical system. The cold stream outlet temperature predicted by the model varied from measured data by a maximum of 8%, with the mean deviation being 3%.

The faults imposed on the physical system and the model includes sensor biases, fluid leaks, unresponsive valves, plugged process lines, and fouling. The steady state change in process variables before and after the fault is used to generate tables that indicate process trends caused by the faults. The set of trend identifiers form a 'fault ID' that can categorize faults as they occur. Results for the physical system and model are presented. The simulation results indicate that unique identifiers exist for most faults. Two simulated faults, tube fouling and plugged tubes, share the same identifiers.

The mechanistic model is used to create data to develop a data-driven model using the Group Method of Data Handling (GMDH) method. The GMDH method is often used in FDI system development when good mechanistic models are not available. The GMDH model matches the mechanistic model well and the resulting FDI system remains useful.

HEAT EXCHANGER HEAT TRANSFER MODEL

The Number of Transfer Units (NTU) method is used to model the heat exchanger performance. Factors used in the calculation include heat exchanger geometry, in conjunction with fluid mass flows and thermo-physical properties. A typical heat exchanger flow configuration is shown in Figure 1.

Heat Transfer Coefficients

A first order energy balance for a simple counter-flow heat exchanger is used as a basis for the heat transfer calculations. The energy balance, in conjunction with the NTU method, gives the heat flow q :

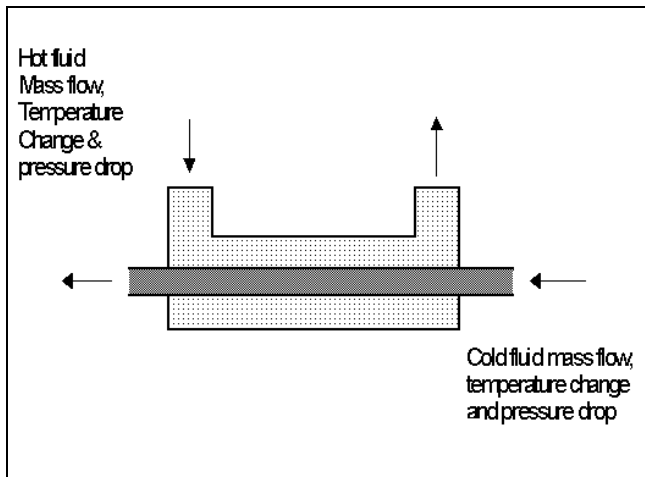


Fig. 1. A typical heat exchanger physical process model.

$$q = \varepsilon \cdot (\dot{m}c_p)_{\min} \cdot \Delta T_{in} \quad (1)$$

$$\varepsilon = f(NTU, (\dot{m}c_p)_{\min} / (\dot{m}c_p)_{\max}, \text{geometry}) \quad (2)$$

$$NTU = \frac{U * A}{(\dot{m}c_p)_{\min}} \quad (3)$$

The formula for effectiveness in a tube and shell heat exchanger in countercurrent flow is given by Todreas and Kazimi (1993):

$$\varepsilon = 2 \left[1 + C_r + (1 + C_r^2)^{1/2} \frac{1 + e^{-NTU(1+C_r^2)^{1/2}}}{1 - e^{-NTU(1+C_r^2)^{1/2}}} \right]^{-1} \quad (4)$$

$$C_r = \frac{(\dot{m}c_p)_{\min}}{(\dot{m}c_p)_{\max}} \quad (5)$$

To determine NTU, the overall heat transfer coefficient, U , given in Eqn. 6, is required to complete the heat exchanger model. Fouling factors are also resident in the overall heat transfer coefficient model. The interior and exterior surfaces may both exhibit fouling represented by factors F_i and F_o , respectively. These factors may be complex functions of operating history, coolant quality and heat exchanger materials.

$$U_i = \frac{1}{\left[\frac{1}{h_i} + \frac{A_i \ln(r_o/r_i)}{2\pi kL} + \frac{A_i}{A_o h_o} + F_i + \frac{A_i}{A_o} F_o \right]} \quad (6)$$

It is important to note the inverse relationship of the heat transfer coefficients. If h_o and h_i differ

significantly, the smaller value will dominate the overall heat transfer.

Calculation of Heat Transfer Coefficients

The primary component of the control loop is the heat exchanger. The exchanger used in the physical system and modeled herein is the model 00283-3 miniature heat exchanger produced by Exergy, Inc. It is a tube-in shell heat exchanger, with a length of 45 cm (17.75 in.), shell diameter 2.54 cm (1 in.), with 37 tubes with a diameter of 2.34 mm (0.094 in.).

The reader is referred to Holman (1997) for the particulars of determining the Nusselt number for various flow situations. Calculation of the Nusselt number allows the tube side heat transfer coefficient, h , to be determined. Table 1 provides values of the tube side heat transfer coefficient.

The shell side heat transfer coefficient involves tubes in cross flow. The flow is heavily dependent on the tube bank geometry, which is described primarily by pitch-to-diameter ratio, P/D. Diagrams of the tube layout indicate a staggered triangular tube array, allowing calculation of P/D. Zukauskus (1972) presents a correlation of the Nusselt number that accounts for a wide variety of Reynolds numbers and property variations.

The model initially takes the inlet temperature and flow rate for both the hot and cold leg. The heat exchanger geometry is in the code along with a property table for water over the appropriate temperature ranges. The thermal conductivity for the heat exchanger material, stainless steel 316L, is also included.

Bulk temperatures are estimated using the NTU method, and an assumed effectiveness of 0.5 is used in the first calculation. Two iterations are performed to update the effectiveness. The number of iterations could be increased to support fluids such as hydrocarbons whose thermo-physical properties change more rapidly over certain temperature ranges.

The bulk temperatures, along with the input, are passed to two sub-functions that calculate the tube and shell heat transfer coefficients. There are provisions in the code for tuning constants on the inner and outer heat transfer coefficients to fit the model to the measured data.

Fouling simulation is accomplished by using R_f values for the shell. The simulation responds to various fouling resistances in a similar fashion when the control system is able to compensate for the degradation in the heat transfer rate. Introduction of a typical fouling resistance value of 0.0001 (m²K)/W is easily detected by the performance monitoring system but did not saturate the controller. The specific behavior of the system during fouling is discussed later.

The overall heat transfer coefficient, U , is calculated next. The NTU model is used in full to calculate the heat transfer in Watts. An energy balance is used to determine the resulting steady state temperatures for the tube and shell side. Table 1 shows typical shell side heat transfer coefficients along with typical tube side heat transfer coefficients used in this study.

Table 1. Calculated Heat Transfer Coefficients

Tube Side		Shell Side	
Re	h_i (W/m ² K)	Re	h_o (W/m ² K)
900	2548	220	4036
1100	2930	270	4546
1300	3300	325	5002
1500	3646	375	5420
1700	3972	430	5807
1900	4297	480	6170
2100	4618	550	6624
Tube Re = 1500		Shell Re = 490	

The shell side heat transfer coefficients tend to be greater than the tube side heat transfer coefficients, but this is not always true. As seen in the table, overlap exists when high tube side flow and low shell-side flow occur. Both heat transfer coefficient models are important for model accuracy. Data from the physical system were used to validate the model. The data and the model results for outlet temperature were compared, and the analysis shows a maximum deviation of 8% with a typical deviation of about 3%. The use of tuning coefficients for the heat transfer coefficients for a particular heat exchanger increases the accuracy, with a maximum error of 3% on the outlet temperatures. Detailed evaluation of the measurement uncertainty has not been conducted to date.

PHYSICAL HEAT EXCHANGER CONTROL LOOP CONFIGURATION

The Temperature-to-Flow Cascade (TFC) uses a PID control device to modulate the cold water flow rate to minimize the error between the hot outlet temperature and the hot outlet temperature set point on the secondary side. Figure 2 illustrates the control loop and associated flow paths.

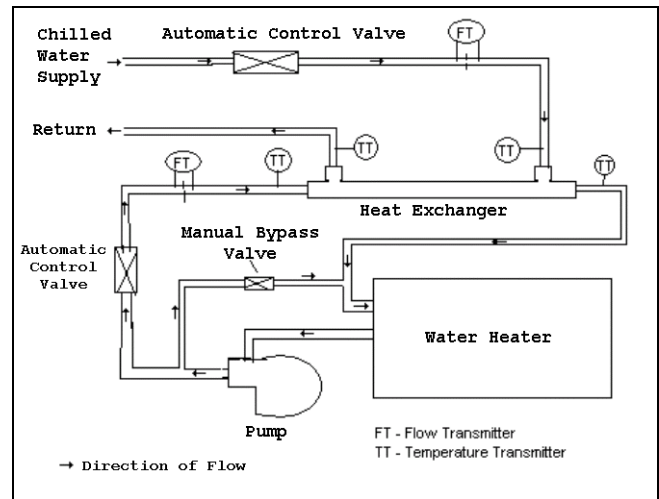


Fig. 2. Physical Heat Exchanger Control Loop

Control Loop Components

The heat exchanger response is simulated using the steady-state NTU method as described in the previous section. The simulation provides the flow rates and inlet temperatures to the heat exchanger code module, which returns the outlet temperatures.

Plumbing for the system is all 1.27 cm (½ inch) copper piping. The pipes are insulated such that the heat loss to the environment is negligible.

Automatic Control Valves are used for both the tube and shell sides. The two control valves are identical. They are model 24588, 1.27 cm (½ inch) butterfly valves made by H.D. Baumann. A control signal can change the position of these valves anywhere between 0% (fully closed) and 100% (fully opened). The hot water valve can be affected by a manual bypass. Correlation between valve position and flow rate were developed in the flow loop for each valve, with the valve/flow delivery pressure set by other system attributes. A transfer function with a step response time constant of 0.1 second is used to place a slight lag in the valve response.

Valve Controllers are present for each control valve and include set point inputs with a PID controller. The PID simulation parameters have the same settings as those in the physical test loop. The Temperature-to-Flow Cascade Controller controls cold water flow to match the hot temperature outlet set point. The PID parameters used match those in the test loop.

Sensors in the simulation include one temperature measurement of the hot fluid outlet measurement and two

flow (hot and cold) measurement of the hot and cold streams. The simulation includes the ability to bias the reported measurements of the sensors. Rosemount 3051 differential pressure transmitters measure the physical model flow rates.

The physical system uses a March pump of 200 Watts (1/5 hp). The pump is modeled as a flow source and operates at a constant speed. The system is treated as a once-through flow path. Water Sources include the hot water heater tank and building chilled water supply. The hot water source is a Rheem Commercial Electric booster heater. The capacity is 38 liters (10 gallons). Electric heating elements heat the water at the rate of 12 kiloWatts. The heating elements are either running at 100% power, or they are turned off. The thermostat is set to 71° C (160° F) for these evaluations. This typically produces a variation of the water temperature between 70° C and 72° C. Water from the building's cooling system is used as the water supply for the cold water side. The temperature of this water is constant over periods of several minutes typical of a single test or data set. However, during a given day it may vary between 13° C and 16.7° C (56° F and 62° F). Figure 3 shows the detailed Simulink model with the output and display modules deleted.

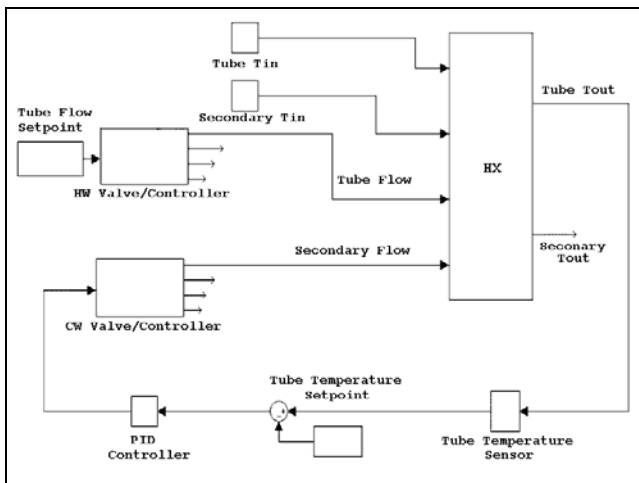


Fig. 3. Simulated Heat Exchanger Control Loop

MODEL AND PHYSICAL SYSTEM PERFORMANCE

The model simulates both normal and faulty operating conditions. The behavior of the model control loop as it attempts to control the hot water outlet temperature is recorded for normal and faulty cases. The normal response is compared to the fault response, and an outcome table is generated.

Figure 4 provides an example of the output for the simulation loop for the system response to a temperature bias fault of 1.7° C (3° F) in the hot fluid at the outlet, with a tube side flow of 0.05 kg/s (0.8 GPM). The bias error was introduced at $t = 1,000$ sec. Note that the plotted process variable $T(h,out)$ is controlled by the Cascade Control Loop.

The simulation was tested against a data set containing 71 different steady-state operation points from the physical system. Several sets of heat transfer correlations were evaluated against the data. The correlations presented here are in the model. The maximum error in exit temperature was 8%, with a typical error of 3%.

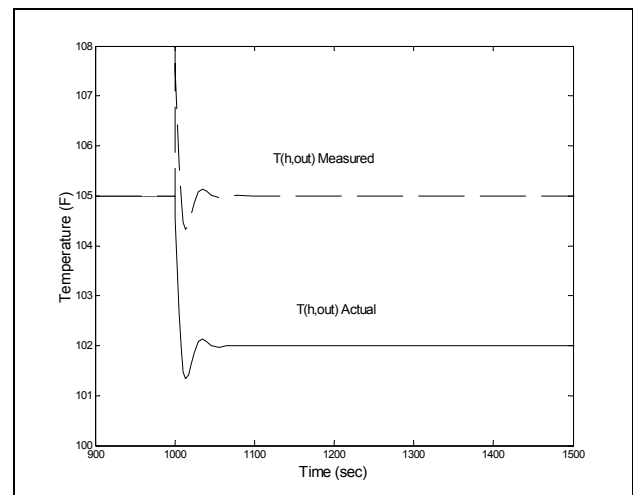


Fig. 4. Measured and actual temperatures of the hot fluid at the outlet $T(h,out)$. A bias fault of 1.7° C (3° F) in the temperature measurement was introduced at $t = 1,000$ sec.

Faults Induced in the Control Loop

The control loop model was developed to support the study of eight device faults:

1. Temperature Sensor Bias (Hot Outlet) – A +1.7° C (3° F) bias is applied to the hot outlet temperature sensor. This impacts the Cascade Controller directly, causing a perceived high temperature, which increases the cold-side flow.
2. Flow Sensor Bias (Hot side) – For the hot side flow sensor, a +0.0094 kg/s (0.15 GPM) bias is applied. The flow controller reads this as high, then decreases the hot flow to the heat exchanger, which also results in the cold flow being reduced to match the temperature setpoint.

3. Flow Sensor Bias (Cold side) – A +0.031 kg/s (0.5 GPM) bias is applied to the cold side flow sensor. The flow controller sees a high flow, first reducing the flow. The need to match the temperature set point then drives the cold flow higher.
4. Fluid Leak (Hot Side) – 30% of the hot-side flow is diverted before entering the heat exchanger. The flow controller compensates for this loss of flow by increasing the set point.
5. Fluid Leak (Cold Side) – 30% of the cold-side flow is diverted before entering the heat exchanger. The flow controller compensates for this loss of flow by increasing the set-point.
6. Stuck/Unresponsive Valve (Hot and Cold Side) – The valve is locked at a position near that (rounded to nearest integer, percentage open) of the pre-fault position. For example, a valve at 24.5% open would lock to 25% open and would not respond to further controller demands.
7. Plugged Process Lines – One or more of the heat exchanger tubes could become plugged during operation, decreasing the available heat transfer area. The simulated fault is 3 of the 37 tubes having completely blocked flow.
8. Heat Exchanger Fouling – Fouling deposits could build up on the heat transfer surfaces on the tubes or on the shell side, thus decreasing the overall heat transfer coefficient. The simulation uses a fouling factor of 0.000 1 (m²K)/W for the shell-side fluid. This fouling factor represents the standard fouling in feed-water under 50 °C (Bott et al. 1997).

System Behavior During Faults

The current analysis considers the detection and isolation of faults during steady-state operation. This allows for a less complex model and provides greater flexibility for data collection. Transient phenomena are currently not included in the analysis.

The FDI system receives process variables from sensors and then begins calculating other process variables, using known relationships. Time averaged data are used. The appropriate period for time averaging depends on the attributes of the system. Table 2 shows the behavior of various process variables and was generated from data taken from the physical heat exchanger loop. A “1” on the outcome table indicates the magnitude of that process variable significantly increased after the fault was initiated. A “-1” indicates the magnitude of the process variable significantly decreases after the fault was initiated. A significant change is considered to be greater than 10% of

the initial steady state value. Table 3 shows the fault responses for the simulation.

Behavior of the System During Fouling

During fouling, the control system in a TFC control loop acts to maintain the set point hot outlet temperature. The hot outlet temperature average over time remains constant unless the controller is saturated. Controller saturation is obvious as the control system sets the cold-water valve to the maximum possible value. For moderate fouling, $R_f = 1 \times 10^{-5}$ to 1×10^{-4} , the controller responds by increasing the cold-water flow, and this is indicated by a rise in flow rate set point, flow rate, cold-water valve position, pressure drop across the cold side and controller demand on the cold-water valve. The controller saturates at R_f equal to 2.2×10^{-4} (m²K)/W. A fouling resistance value equal to 1×10^{-4} (m²K)/W is used as a fault condition to test the performance monitoring system.

Alternate Fault Detection and Isolation Method

The fault detection system focuses on signal analysis and trends in the measured sets of process variables. The FDI system presented in the previous section functions by using mechanistic models to verify sensor outputs in the control loop. Often data driven modeling methods are used in the development of FDI systems since the expertise required to develop physical models may not be available, or the cost for development of such models may be excessive. The Group Method of Data Handling (GMDH) can be used to predict the state of the system given the time-averaged input from various sensors. The GMDH is a data-driven modeling method that approximates a given variable y (output) as a function of a set of input variables $\{x_1, x_2, \dots, x_m\}$ that are closely related to y (Ferreira and Upadhyaya, 1999). The general form is referred to as the Kolmogorov-Gabor polynomial and is given by,

$$y = a_0 + \sum_{i=1}^m a_i x_i + \sum_{i=1}^m \sum_{j=1}^m a_{ij} x_i x_j + \sum_{i=1}^m \sum_{j=1}^m \sum_{k=1}^m a_{ijk} x_i x_j x_k \dots \quad (7)$$

The details of the algorithm are given in Ferreira and Upadhyaya, 1999.

The GMDH input needs at least three input variables. For the cases with insufficient input ‘pseudo-variables’ must be created to fill in. These pseudo-variables are simple variants of the process variables, such as $\sin(x_1)$ or x_1/x_2 , where x_1 and x_2 are process variables. The GMDH algorithm determines this relationship and can accept the limited input. GMDH error depends on the training data available; in one representative test case the error does not exceed 2.5%.

Seven process variables from the heat exchanger control loop were used as inputs. Table 4 shows the variables and the corresponding inputs.

Table 4. GMDH Prediction Variables

Predicted Variable	Input Variables
T(h,out)	T(h,in), T(c,in), Flow(c), Flow(h)
T(c,out)	T(h,in), T(c,in), Flow(c), Flow(h)
SP(F,c)	T(h,in), T(c,in), SP T(h,out), Flow(h)
Flow(c)	VP(c), DelP(c)
VP(c)	SP(F,c)
Flow(h)	VP(h), DelP(h)
VP(h)	SP(F,h), Flow(h)

The heat exchanger control loop mechanistic model is used to generate many cases of faulty operation. One hundred and twenty eight (128) cases of initial operating conditions were submitted to seven different faults, for a total of 896 cases. The GMDH algorithm then analyzed all the data, flagging the predicted process variables as high, expected, or low. The algorithm graded each case, looking at the reported process variables and making predictions. The

prediction results were graded with a +1, 0 or -1. A high flag (+1) corresponds to a predicted value greater than 110% of the reported value. An expected flag (0) is used when the prediction and reported values are within 10% of each other. The low flag is set when the prediction is below 90% of the reported value. Table 5 shows the GMDH fault identifiers for the simulated faults designed to match the physical test loop.

Several faults have multiple fault indicator patterns. For all faults, any unique set of fault indicator flags that occurred more than once was listed on this table. Overall, the algorithm did an acceptable job of identifying faults. The flags indicated a fault with a success rate of roughly 80%, with most of the errors due to the stuck hot water control valve. These results are also complicated by occasional false positive reports of fault free operation.

CONCLUSIONS

A mechanistic model for a Temperature-to-Flow Cascade loop is developed and validated using data from a physical system. The mechanistic model is used to simulate the operation of the physical system during faulty operation. The faults imposed on the physical system and the model include sensor biases, fluid leaks, unresponsive valves, plugged process lines, and fouling. The mechanistic model

Table 5. GMDH Fault Identifiers

Fault	Confidence	T(h,out) M	T(c,out) (°F)	SP(F,c) (GPM)	Flow(c) M	VP(c) (%)	Flow(h) M	VP(h) (%)	DelP(h) (psi)	DelP(c) (psi)
T(h) Sensor Bias	91%			-1						
		-1		-1						
F(h) Sensor Bias	100%			1			-1	-1		
		1		1			-1	-1		
			1	1			-1	-1		
		1	1	1			-1	-1		
F(c) Sensor Bias	93%			-1	-1	1				
		-1		-1	-1	1				
			-1	-1	-1	1				
		-1	-1	-1	-1	1				
HW Leak	100%						-1	-1	1	
		1					-1	-1	1	
			1				-1	-1	1	
		1	1				-1	-1	1	
CW Leak	100%				1	-1				
					1	-1				Any
HW Stuck Valve*	0%									
CW Stuck Valve	100%					1				
				Any		1				

*No sufficient fault identifiers

matches the physical system performance well and is used to create a Fault Detection and Isolation (FDI) algorithm for the system.

The mechanistic model is also used to create data for the development of a data driven model based on the Group Method Of Data Handling (GMDH). The GMDH method is more commonly employed for developing an FDI system using system data when a good mechanistic model is not available. The simulated fault identifiers from the GMDH model match with the physical system fault identifiers for several of the faults. The sensor bias faults match very well. Discrepancies appear for the fluid leaks and unresponsive valve faults. It is important to note that time-averaging rule-based techniques may not detect fouling due to the long time scales involved. The GMDH method is a predictive method and could detect fouling if adequate heat exchanger operational data is collected for a clean system. GMDH is suited for this purpose as it collects data and trains on a continuous basis.

Acknowledgments

This research project was sponsored by Emerson Process Management, Performance Technologies Division, Eden Prairie, MN, under a contract with The University of Tennessee, Nuclear Engineering Department.

NOMENCLATURE

A	Heat transfer area (m^2)
C_p	Specific Heat, $kJ/(kgK)$
C_r	Ratio of flow heat capacity, dimensionless
F	Fouling Factor (m^2K/W)
h	Heat transfer coefficient (W/m^2K)
k	Thermal Conductivity (W/mK)
L	Tube length (m)
\dot{m}	Mass flow (kg/s)
NTU	Number of Transfer Units, dimensionless
q	Heat flow (W)
r	Radius (m)
Re	Reynolds Number, dimensionless
R_f	Fouling resistance ($m^2\text{°C}/W$)
T, t	Temperature (°C or K)
U	Overall heat transfer coefficient (W/m^2K).
ϵ	Heat exchanger effectiveness
μ	Dynamic viscosity ($kg/m\ s$)
ΔT_m	Log mean temperature difference (°C or K)

Subscripts

<i>i</i>	internal to the tube
<i>in</i>	inlet
<i>m</i>	mean
<i>o</i>	external to the tube.

out exit

w properties evaluated at the wall temperature.

REFERENCES

- Bott, T. R. et al., *Understanding Heat Exchanger Fouling and Its Mitigation*, Engineering Foundation Conference Proceedings, Pascoli, Italy, 1997.
- Ferreira, P. B. and B.R. Upadhyaya, "On-line Fault Monitoring and Isolation of Field Devices Using Group Method of Data Handling," Proc. MARCON 99, Vol. 2, pp. 79.01-79.15, May 1999.
- Holman, J. P. *Heat Transfer*, 8th Ed., McGraw-Hill, New York, 1997.
- Petukhov B. S. "Heat Transfer and Friction in Turbulent Pipe Flow with Variable Physical Properties," Edited by J.P. Hartnett, *Advances in Heat Transfer*, Academic Press, 1970.
- Todreas, N. E. and M.S. Kazimi, *Nuclear Systems I, Thermal Hydraulic Fundamentals*, Taylor & Francis, 1993.
- Zukauskus, A. A., *Heat Transfer from Tubes in Crossflow. Adv. Heat Transfer*, vol. 8, pp. 93-160, 1972.

Table 2. Behavior of process variables and control functions for various fault conditions (EPM data)

Fault	T(c,out) (°F)	SP(F,c) (GPM)	Flow(c) (GPM)	VP(c) (%)	CD(c) (%)	SP(F,h) (GPM)	Flow(h) (GPM)	VP(h) (%)	CD(h) (%)	DelP(h) (psi)	DelP(c) (psi)	Fault ID
T(h,out) Bias	-1	1	1	1	1						1	1
Flow(h) Bias	1	-1	-1	-1	-1			-1	-1	-1	-1	2
Flow(c) Bias		1	1	-1	-1							3
HW Leak	1	-1	-1	-1	-1			-1	-1	-1	-1	4
CW Leak 1*	1	1	1	1	1							5
CW Leak 2		1	1	1	1							5A
CW Valve		-1	1	1	-1						1	6
HW Valve		1	1	1	1				1		1	7

*CW Leak 1 results in cascade control saturation

Table 3. Fault Outcome Table for Simulations

Fault	T(c,out) (°F)	SP(F,c) (GPM)	Flow(c) Measured	VP(c) (%)	CD(c) (%)	Flow(h) Measured	VP(h) (%)	CD(h) (%)	Del P(h) (psi)	Del P(c) (psi)	Fault ID
T(h) Bias (+)	-1	1	1	1	1					1	S1
T(h) Bias (-)	1	-1	-1	-1	-1					-1	S2
F(h) Bias (+)	1	-1	-1	-1	-1		-1	-1	-1		S3
F(h) Bias (-)	-1	1	1	1	1		1	1	1	1	S4
F(c) Bias (+)		1	1								S5
F(c) Bias (-)		-1	-1								S6
HW Leak							1	1	-1	-1	S7
CW Leak				1	1						S8
HW Stuck Valve(+)		1	1	1	1	1		-1	1	1	S9
HW Stuck Valve (-)		-1	-1	-1	-1	-1		1	-1	-1	S10
CW Stuck Valve (+)	-1	-1	1		-1					1	S11
CW Stuck Valve (-)	1	1	-1		1					-1	S12
HX Fouling	-1	1	1	1	1					1	S13
Plugged Tubes	-1	1	1	1	1					1	S13